PAPER • OPEN ACCESS

Modelling of Natural Convective Heating of a Standard Wet Brick for Oven Energy Consumption Tests

To cite this article: M. Lucchi *et al* 2020 *J. Phys.: Conf. Ser.* **1599** 012033

View the article online for updates and enhancements.

Modelling of Natural Convective Heating of a Standard Wet Brick for Oven Energy Consumption Tests

M. Lucchi[1], N. Suzzi[2] and M. Lorenzini[1]

[1] DIN – Department of Industrial Engineering, University of Bologna, via Fontanelle 40, 47121 Forlì, Italy

[2] DPIA – Dipartimento Politecnico di Ingegneria ed Architettura, University of Udine, Via delle Scienze 206, 33100 Udine, Italy

Corresponding author e-mail: marco.lorenzini@unibo.it

Abstract. The environmental impact of buildings is directly influenced by low-efficiency appliances like electric ovens. Their energy class is estimated through a test prescribed by the EN 60350 European standard, where a wet clay brick is heated under set conditions and the energy consumption is measured; throughout the test, particular attention is devoted to the control of air temperature. In this work, a transient model of the oven suitable for control design was realized including the heat and mass transfer within the brick. A lumped-parameter approach was used to ensure good predictive properties and low computational cost. The dynamics of the cavity air and the Pt500, which is used in normal operation to maintain the desired set point, was also included in the model. Model parameters were determined through an optimization procedure based on the experimental data collected during energy consumption tests with the oven in natural convective heating mode. The model was then validated. Good results were obtained in the prediction of both temperature and heating time.

1. Introduction

Household appliances such as electric ovens contribute up to 25% to the environmental impact of buildings [1]. The energy class of an electric oven is obtained by means of a test regulated by the EN 60350 standard, [2], where the energy consumption in heating a wet clay brick with set properties is measured (see Section 2). Among others, the standard prescribes the air temperature in the cavity to be properly controlled during the test, thus making the research on innovative control strategies of current interest. Because of the usefulness of dynamic models in control design, this work focuses on the development of a suitable low-order control-oriented model to simulate the transient behaviour of the oven during the energy consumption test, with the aim of predicting the main temperatures of the cavity and the brick and the time needed to heat the latter to a prescribed temperature. In the literature, numerical approaches spanning different levels of complexity can be found as regards electric ovens. Among the simplest, the work by Abraham and Sparrow can be cited, [3], where the time trend of the temperature of a thermal load is predicted through a simple energy balance. More accurate but also more computationally expensive models generally use the CFD approach, like in [4], where Mistry et al. analysed the transient heat transfer in natural convection during broiling and baking cycles in electric ovens. Similar to what presented by the authors in [5]-[6], the lumped-parameter approach based on the thermoelectric analogy was adopted in this work, since it represents the best trade-off between accuracy and simplicity, thus allowing to obtain good predictive capabilities at low computational cost. The use of such an approach in the transient thermal analysis of ovens is widespread in literature. For example,

in [7] a transient lumped-parameter model of a professional oven was developed without considering a thermal load. Good agreement between numerical and experimental data was obtained, although the validation was carried out at a single setpoint. In [8], Laboreo et al. developed a lumped-parameter model based on the thermoelectric analogy, including the dynamics of the wet brick for the energy consumption test. However, the authors did not provide any result on the temperature predicted at the brick's core (which is essential for the test duration) and no information could be extrapolated from the model on the temperature of the air around the brick and the temperature of the sensor used to maintain the desired set point. Differently from [8], in this work a certain level of discretization was introduced in the model in order to predict the main temperatures within the cavity, like that of the air and the Pt500 used by the oven control board as a temperature feedback. The heat and mass transfer within the brick was also included, highlighting good results both in the prediction of the brick temperatures (at the core and at the surface) and of the heating time. The choice of a lumped-parameter approach was dictated by the ultimate goals of the model (correct prediction of the oven and brick temperatures and of energy consumption, with no need for a detailed temperature mapping within the oven or inside the brick), which should be reached with the minimum computational costs. The natural convective heating mode was investigated and experimental data were used to identify model parameters, giving the model a "grey-box" nature, and for the validation at different temperature set points.

2. Characterization of the oven energy consumption

In the first phase of the test, a 230 mm x 114 mm x 64 mm clay brick (see Fig. 1 (a)) with a weight of 920 ± 75 g is soaked in cold water for at least 8 h, until a mass increment of 1050 ± 50 g and a core temperature of $5\pm2°C$ is reached. The brick is then heated in the oven until a temperature increment of 55 K is reached at its core, and the electric energy consumption together with the water mass loss are registered. The test is repeated at different temperature set points T_{set} and under different heating conditions; the energy class is then determined through a dedicated correlation given by the standard. For the natural convective heating mode, which is the focus of this work, the set points to be considered, intended as temperature increment above the ambient ΔT_{set}, are 140-180-220 K. Since the ambient temperature T_{AMB} has to be maintained at $23\pm2°C$ and considering a tolerance of ±10 K on ΔT_{set}, the set points investigated are 160-200-240°C.

3. The oven

The appliance used during the experimental campaign is an "Electrolux - EOB6850BOX" commercial household oven with a $72\ dm^3$ cavity, and equipped with a $1900\ W$ ring heater (RH), a 2300 W top heater (TH) and a 1000 W bottom heater (BH). In the natural convective heating function investigated, only the top and bottom heaters are activated. Temperature control for the air within the cavity is obtained through a Pt500 probe located at one of the cavity corners, as shown in Fig. 1 (b), which shows a schematization of the oven highlighting the main elements. During the tests, in order to characterize the thermal behaviour of the cavity, the temperatures of the walls at different location, of the air, of the glass door and of the heaters have been measured through k-type thermocouples in addition to the temperature sensed by the Pt500. In particular, to get an estimation of the temperature at the oven centre regardless of the presence of the brick, four thermocouples were placed perpendicular to the grid onto which the brick lies, at a distance of about 2 cm from its sides. Moreover, the electric power absorbed by the heaters is also registered through four LogiLight EM0002 power meters (one for each heater and one for the overall power consumption). As shown in Fig. 1 (a), the brick is equipped with two thermocouples to measure its temperature at the core (located at a 32 mm depth) and with six thermocouples placed at its sides to estimate its surface mean temperature. A detailed description of experimental setup and the uncertainty analysis can be found in [5], [9-11].

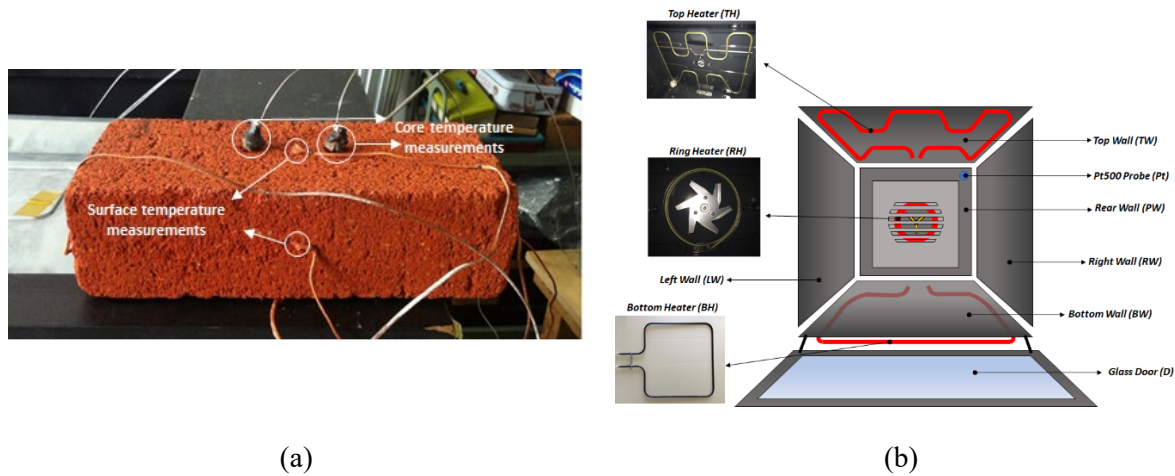(a)   (b)

Figure 1: (a) detail of the clay brick equipped with k-type thermocouples for the measurement of the core and surface temperature; (b) sketch of the oven with the main elements of the cavity.

4. Model

The model was set up using a lumped-parameter approach based on the thermoelectric analogy, in order to obtain a low computational cost suitable for control design. The cavity was discretized into eleven thermal nodes, comprising the cavity air (OC), the Pt500 (Pt), the five cavity walls and the glass door (see Fig. 1(b) for specific nomenclature), the ring heater (RH), the top heater (TH) and the bottom heater (BH). Although it is not activated in the natural convective mode, the ring heater is included in the model to allow analysis on the forced convective functions. The energy balance for a generic node i of the cavity can be written as:

$$C_i \frac{dT_i}{d\tau} = \sum_{j=1}^{n}(\dot{Q}_{ij} + \dot{Q}_{ij}^{rad}) + \dot{P}_{el\,i} \qquad (1)$$

In Eq. (1), C_i (J/°C) is the thermal capacity, T_i(°C) is the temperature, $\dot{Q}_{ij}$ (W) and $\dot{Q}_{ij}^{rad}$ (W) are the convective-conductive and the radiative heat transfer respectively and $\dot{P}_{el\,i}$(W) the electric power absorbed (only for the active heaters). $\dot{Q}_{ij}$ can be written as a function of the thermal conductance G_{ij} and the temperature difference between nodes i and j as $\dot{Q}_{ij}=G_{ij}(T_j-T_i)$. The radiative heat transfer $\dot{Q}_{ij}^{rad}$(W) between two nodes can be expressed as a function of the Stefan-Boltzmann constant σ, of the radiative thermal conductance G_{ij}^{rad} and the temperatures in kelvin as $\dot{Q}_{ij}^{rad} = G_{ij}^{rad}\sigma(T_j^4 - T_i^4)$. The term G_{ij}^{rad} is a function of the surface emissivities ε_i and ε_j, the emission areas A_i and A_j and the view factor F_{ij}; in particular it can be written as $G_{ij}^{rad}=1/\left(\frac{1-\varepsilon_i}{\varepsilon_i A_i} + \frac{1}{F_{ij}A_i} + \frac{1-\varepsilon_j}{\varepsilon_j A_j}\right)$. A detailed discussion on the significance and determination of G_{ij} is given in [12]; here it should be remarked that the values obtained do not necessarily resemble those which might be determined by hand computation using the usual values for the convective coefficients and the emissivities of similar surfaces. Yet, this is of no consequence to the results of this study, where prediction of surface/cavity temperatures and energy consumption were the goals. With the exception of the terms connecting the walls, the top heater (radiation) and the cavity air (convection) to the brick surface, a term connecting the Pt500 to the rear wall, a radiative term between the top heater and top wall and a radiative term between the bottom heater and the bottom wall, all the other thermal connections in the cavity are the same as those presented in [5] for the linear model of the oven in natural convective heating mode without load. In fact, the presence of the brick in the cavity decreases the view factors among the walls and the heaters, thus making this contribution negligible.

The model of the brick is still based on a lumped-parameter approach to maintain a certain degree of simplicity and includes both the heat diffusion and the water loss. The water drip effect was neglected. As shown in Fig. 2, the brick was discretized into two nodes. The first one is associated to its outer part (BrS), which is thermally connected to the walls and the top heater through radiative terms and to the cavity air through a convective term; the second one is the brick's core (BrC), from which water diffuses towards the surface. As a simplifying assumption, the mass flow rate of water spreading through the brick was assumed equal to the water evaporation rate. Subsequently, since the water is supposed to flow from the core towards the surface, the thermal capacity of the core decreases dependently from the evaporated mass of water $m_{w\,ev}$. In turn, the thermal capacity of the outer part is assumed constant.
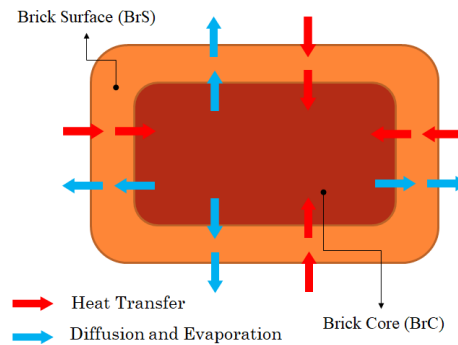

Figure 2: discretization of the brick.

Calling m_{dry}(kg) the mass of the dry brick, c_{dry} the specific heat capacity of the dry brick $(800 J\cdot kg^{-1}\cdot K^{-1})$, m_w the total mass of water absorbed, c_w the specific heat capacity of water, $r = m_{BrS}/m_{Br}$ the ratio between the mass of the brick associated to the outer part m_{BrS} and its total mass m_{Br}, $\dot{m}_w$ the mass flow rate of the evaporating water and Δh_{lv} the enthalpy of vaporization at a mean brick's core temperature of $30°C$, the energy balance for the brick' surface and core can be expressed through Eqs. (2)-(3).

$$r\left(m_{dry}c_{dry}+m_w c_w\right)\frac{dT_{BrS}}{d\tau} = \dot{Q}_{OC\,BrS} + \dot{Q}_{BrC\,BrS} + \dot{Q}^{rad}_{TH\,BrS} + \dot{Q}^{rad}_{TW\,BrS} + \dot{Q}^{rad}_{BW\,BrS} + \dot{Q}^{rad}_{RW\,BrS} +$$
$$+\dot{Q}^{rad}_{LW\,BrS} + \dot{Q}^{rad}_{PW\,BrS} + \dot{Q}^{rad}_{D\,BrS} - \dot{m}_w\Delta h_{lv} \tag{2}$$

$$\left[(1\text{-}r)\left(m_{dry}c_{dry}+m_w c_w\right)\text{-}m_{w\,ev}c_w\right]\frac{dT_{BrC}}{d\tau} = \dot{Q}_{BrS\,BrC} \tag{3}$$

The mass of the evaporated water is evaluated by means of a mass balance on the brick's core, as reported in Eq. (4).

$$\frac{dm_{w\,ev}}{d\tau} = \dot{m}_w \tag{4}$$

The evaporation rate of water $\dot{m}_w$ is calculated through Eq. (5), often adopted in the design of drying plants, [13], where $D(kg\cdot s^{-1}\cdot m^{-2}\cdot Pa^{-1})$ is a coefficient depending on the air flow around the brick, $A_{Br}(m^2)$ is the brick outer surface, $P_{BrS}(Pa)$ is the water saturation pressure at T_{BrS} and $P_{v\,air}(Pa)$ is the partial pressure of water vapour in the cavity. At this stage of the work, $P_{v\,air}$ was assumed constant with a value corresponding to a 50% relative humidity in ambient air at $23°C$. The instantaneous value of P_{BrS} was calculated through a fitting polynomial based on the property tables of water: this procedure yield Eq. (6), where T_{BrS} is in degrees Celsius.

$$\dot{m}_w = DA_{BrS}(P_{BrS}\text{-}P_{v\,air}) \tag{5}$$

$$P_{BrS} = 0.001 T^4_{BrS} - 0.0313 T^3_{BrS} + 3.4453 T^2_{BrS} + 19.748 T_{BrS} + 671.54 \tag{6}$$

The model was implemented in Matlab/Simulink® and a fixed-step Runge-Kutta method (ode4) was used as a solver, with a time-step of $1\,s$. In the parameter identification, the simulation spanned the whole duration of the experimental test, whilst in the model validation the time was manually tuned in order to get a $55\,K$ temperature increment at the brick core.

5. Parameter identification

Model parameters were determined on the basis of experimental data measured during a test at $T_{set}=200°C$ while the sets of data measured at $T_{set} = 160°C$ and $T_{set}=240°C$ were subsequently used in the model validation. Thermal capacities C_i and convective-conductive conductances G_{ij} were determined through an optimization procedure with variable time-step based on the Non-Linear-Least-Squares method as detailed in [5]. Radiative thermal conductances G_{ij}^{rad} were calculated as presented in Section 4, assuming emissivities for the walls, the glass door, the heaters and the brick equal to 0.11, 0.13, 0.9 and 0.6 respectively, and estimating the view factors F_{ij} through the Matlab® script proposed by Lauzier for plane surfaces [14]. At the beginning of the test, the mass of the dry and wet brick m_{dry} and m_{Br} were measured, and the total amount of absorbed water m_w was subsequently determined as their difference. The diffusion coefficient D was estimated integrating Eq. (5) and using the experimental values of $m_{w\,ev\,tot}$ and P_{BrS}.

6. Results

In this section, the temperatures predicted by the model for the main elements of the cavity (oven centre and Pt500) and the brick are compared to experimental data.
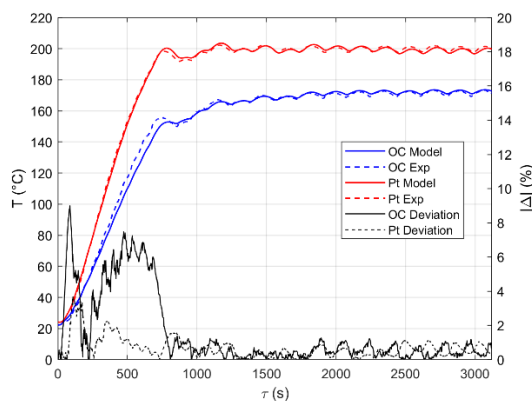

Figure 3: comparison between predicted and experimental temperature of the oven centre and the Pt500 in the parameter identification ($T_{set}=200°C$).
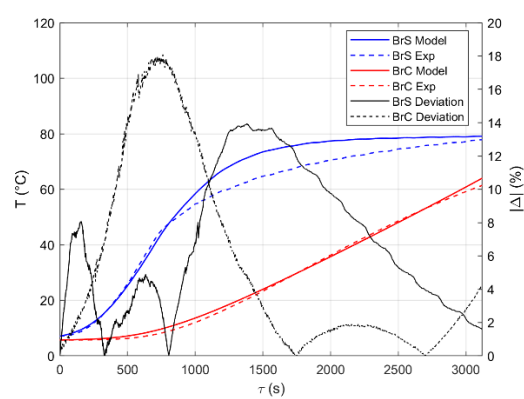

Figure 4: comparison between predicted and experimental temperature of the brick's core and surface in the parameter identification ($T_{set}=200°C$).

The results obtained in the parameters identification ($T_{set}=200°C$) are presented in Fig. 3 for the oven centre and the Pt500. The highest deviations are obtained in the beginning of the simulation, where temperatures are relatively low, showing a maximum of 9% for the oven centre and a maximum lower than 4% for the probe. Once steady state conditions are reached, the deviation remains under 1%. The parameters identification procedure led to satisfactory results also for the temperature at the core and the surface of the brick, as shown in Fig. 4. The maximum deviation obtained for the brick surface is lower than 14% while for the core a maximum of about 18% is shown, mainly because of its very low temperature during the first minutes of the test. It can be noticed that the core temperature of the brick continues to increase although that of its surface approaches a stationary value: this is consistent with the real process (the brick is basically dry, but conduction from the outer surface to the core has not

reached steady state yet), and is not significant for the energy consumption test, which stops at once when an increase in core temperature of 55K from its starting value has been achieved. Good results are obtained also in terms of heating time, for which a percentage difference of 3.69% (corresponding to a time difference of 115 s) between the predicted and the experimental values is also highlighted. In particular, since the curve of the predicted temperature of the core lies above the experimental trend the heating time is slightly underestimated.
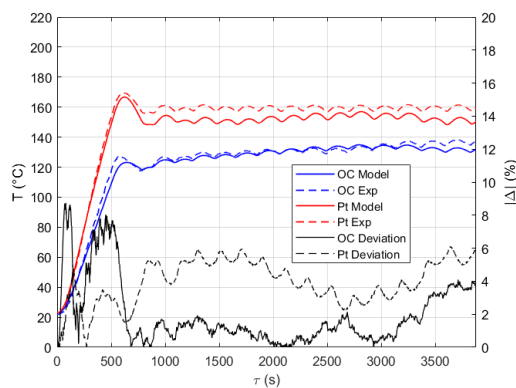

Figure 5: comparison between predicted and experimental temperature of the oven centre and the Pt500 in the validation at $T_{set} = 160°C$.
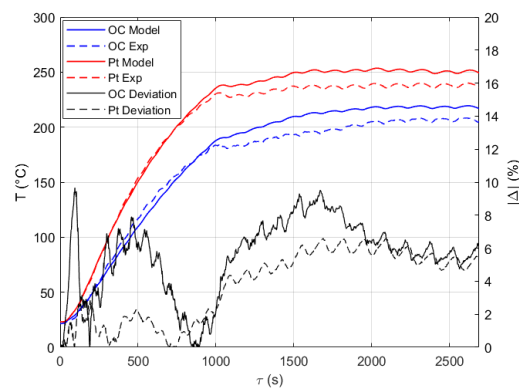

Figure 6: comparison between predicted and experimental temperature of the oven centre and the Pt500 in the validation at $T_{set} = 240°C$.

The time trends obtained for the temperature of the oven centre and the Pt500 in the validation procedures at $T_{set}=160°C$ and $T_{set}=240°C$ are plotted in Fig. 5 and 6 respectively. In the test at 160°C, the maximum percentage deviation during the heating up of the cavity is around 8% for both the oven centre and the Pt500; values lower than 4% and 6% are then obtained in the steady state regime for the air and the probe respectively. Slightly higher but still acceptable deviations can be noticed in the test at $T_{set}=240°C$, with values always lower than 10%. The more pronounced deviation at the high temperature set point can be due to an underestimation of the evaporative heat loss; this aspect of the model could be improved introducing a temperature dependence of the water evaporation coefficient D and the water vapour partial pressure $P_{v\,air}$ in the cavity air.
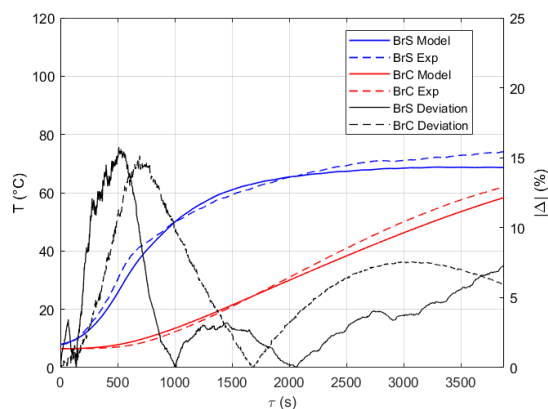

Figure 7: comparison between predicted and experimental temperature of the brick's core and surface in the validation at $T_{set} = 160°C$.
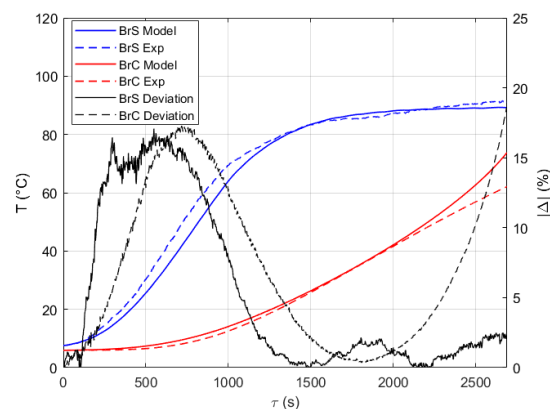

Figure 8: comparison between predicted and experimental temperature of the brick's core and surface in the validation at $T_{set} = 240°C$.

Figures 7 and 8 show the results obtained in the validation tests for the temperature at the brick's core and surface, confirming more than satisfactory forecasting capabilities for the model. In the test at

T_{set}=160°C the maximum percentage deviation is obtained for both the brick's core and surface in the first 750 s with values around 15%; the heating time is also slightly overestimated with a percentage deviation of about 7.01%, corresponding to a time difference of 272 s. Considering the validation test at T_{set}=240°C, a deviation slightly above 15% is highlighted for the temperatures of the brick in the first 750 s; for the brick's core, the deviation tends to increase in the last seconds of the test, with values still lower than 20%. In this case the heating time is underestimated with a 7.54% deviation, which corresponds to a time difference of 203 s.

7. Conclusions

In this work, the transient model of an electric domestic oven and the wet clay brick used for the energy consumption test was presented. The lumped-parameter approach based on the thermoelectric analogy was adopted to ensure good forecasting properties whilst maintaining a low computational cost. Heat and mass transfer within the brick was considered, including the variation of its thermal capacity in time. Experimental data measured in energy consumption tests carried out in natural convective heating mode were used both in the parameter identification and in model validation. The model showed good predictive capabilities in terms of both predicted temperature and brick heating time. The inclusion in the model of the dynamic behaviour of both the cavity air and the Pt500 makes the model suitable for control design. Among possible improvements, the impact on model reliability of a time-dependent vapour partial pressure in the cavity will be investigated by the authors. Further, in future works the control theory will be applied to the model in order to obtain a so-called "control-synthesis model".

8. References

[1]   Hoxha E and Jusselme T *2017 Sci. Total Environ.* **596-597** pp 405-416
[2]   CENELEC *2013 EN 60350-1 Household electric cooking appliances Part 1: Ranges, ovens, steam ovens and grills. Methods for measuring performance (latest version including all amendments)*
[3]   Abraham J and Sparrow E *2004 J. Food Eng.* **62** pp 409-415
[4]   Mistry H, Ganapathisubbu S, Dey S, Bishnoi P and Castillo J 2006 *Appl. Therm. Eng.* **26** pp 2448-2456
[5]   Lucchi M and Lorenzini M *2019 Appl. Therm. Eng.* **147** pp 438-449
[6]   Lucchi M, Lorenzini M and Roberti G *2018 36th UIT Heat Transfer Conference – Catania*
[7]   Burlon F, Tiberi E, Micheli D, Furlanetto R and Simonato M *2017 Energy Procedia* **126** pp 2-9
[8]   Ramirez-Laboreo E, Sagues C and Llorente S *2016 Appl. Therm. Eng.* **93** pp 683-691
[9]   Lucchi M, Lorenzini M and Di Paola V *2018 36th UIT Heat Transfer Conference – Catania*
[10] Lorenzini, M. Morini, G.L., Henning, T. Brandner J.J. 2009 *Int. J.of Thermal Sciences*, **48**(2) pp. 282-289
[11] Lorenzini, M., Fabbri, G., Salvigni, S. *2007 Appl. Therm. Eng.* **27** (5-6), pp. 969-975.
[12] Lucchi, M., Suzzi, N., Lorenzini, M. *2019 Appl. Therm. Eng.* **161**, art. no. 114117.
[13] Bergman T, Lavine A, Incropera F and Dewitt D *2011 Fundamentals of heat and mass transfer* (Hoboken: John Wiley & Sons)
[14] Lauzier N https://it.mathworks.com/matlabcentral/fileexchange/5664-view-factors? focused=5060891&tab=function," [Online]. [Accessed 16 January 2018]